Observation of Quantum Fluctuations of Charge on a Quantum Dot

D. Berman,* N. B. Zhitenev,[†] and R. C. Ashoori

Department of Physics, Massachusetts Institute of Technology, Cambridge, Massachusetts 02139

M. Shayegan

Department of Electrical Engineering, Princeton University, Princeton, New Jersey 08544
(Received 30 March 1998)

We have incorporated an aluminum single electron transistor directly into the defining gate structure of a semiconductor quantum dot, permitting precise measurement of the dot charge. Voltage biasing a gate draws charge from a reservoir into the dot through a single point contact. The dot charge increases continuously for large point contact conductance and in single electron steps with the contact nearly closed, and we measure the corresponding capacitance line shapes. The line shapes are not typical of lifetime or thermal broadening but fit well to predictions of perturbation theory. [S0031-9007(98)08102-2]

An isolated puddle of electrons (a quantum dot) holds a discrete and measurable number of electrons. This remains the case even if the puddle is weakly coupled to an electron reservoir. The energetics of charging of quantum dots can be probed by addition spectroscopy, i.e., by precise measurement of the energy needed to add or remove an electron [1]. Quantum mechanical tunneling between the dot and the reservoir gives rise to line broadening in the charging spectra. For many systems, the coupling of a single state to a continuum of states produces a "lifetime broadening" of the state energy. For instance, spectra of excited states in atoms display a characteristic Lorentzian line shape broadening arising as a result of coupling to a continuum of electromagnetic modes. In quantum dots, electrons may enter or depart from states within the dot by means of tunneling to a continuum of states within one or more electron reservoirs. Unlike the line shapes in optical spectra of atoms, the line shape of quantum dot levels originates essentially in a many-body interaction between electrons in the dot and in the reservoirs.

As the tunnel barrier conductance, G, between the quantum dot and the macroscopic leads is increased above $2e^2/h$, quantum charge fluctuations between the dot and the lead destroy charge quantization on the dot [2]. A thorough physical description of this effect has only recently been proposed [3–5].

Measuring the charge or the capacitance of a dot in a single-terminal geometry provides the most direct information about charge fluctuations and the effect of the dot-environment interaction on the charging states of the dot. However, transport experiments have been the first to address the issue of dot-environment coupling. Foxman *et al.* [6] examined the line shape of conductance peaks with increasing coupling of the dot to the leads and found good agreement with Lorentzian broadening. To analyze the charging line shapes in the dot for a broad range of coupling strengths, conductance measurements are poorly suited, being complicated by interactions between contacts in a multiterminal geometry [7].

Previous experiments have addressed the issue of charging line shapes. Researchers employed a semiconductor electrometer [8] to observe the effect of charge fluctuations. They modeled their results by a reduction of the charging energy with increasing coupling. In another experiment [9], effects of electron tunneling between double dots were analyzed with a similar formalism as we use in our line shape investigation [10].

We have developed an experiment that probes the capacitance line shape of a quantum dot with unprecedented sensitivity. The line shapes deviate substantially from previously employed fitting forms [6,8] and are best described for all coupling strengths by the theory developed recently by Matveev [3–5].

We measure the capacitance line shapes of a quantum dot with only one contact to a charge reservoir. The quantum dot is electrostatically defined in a two-dimensional electron gas (2DEG) of a AlGaAs/GaAs heterostructure. The 2DEG is about 1200 Å below the surface with a carrier concentration of 1×10^{11} cm^{-2}. Measurements were performed on six different samples, each yielding very similar results, and here we present detailed data from one of them. A micrograph of the structure is shown in Fig. 1a. The estimated area of the quantum dot is about 0.5 μm^2, which corresponds to an energy level spacing of 7 μeV. We measured the average charging energy of the dot to be $U = e^2/2C_\Sigma = 0.23$ meV from temperature dependence of the capacitance peaks for high tunneling barriers. Here, $C_\Sigma = 348$ aF (aF = 10^{-18} F) is the total capacitance of the quantum dot.

In our experiment, a single-electron transistor (SET) detects charge on the quantum dot with extremely high sensitivity. The metal SET is fabricated [11] with Al-Al$_2$O$_3$-Al tunnel junctions [12] and incorporated directly into one of the leads defining the dot.
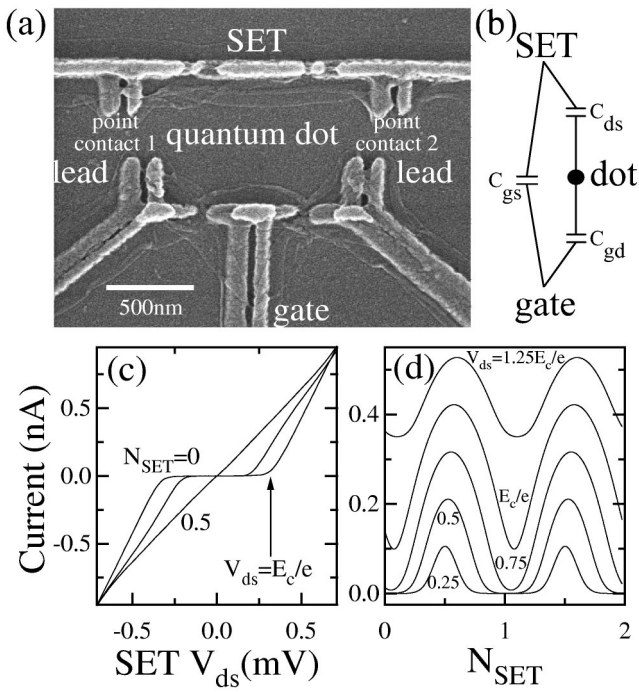
FIG. 1. (a) Micrograph of measurement setup. The leads are made of aluminum by shadow evaporation. The area of the quantum dot is approximately $0.5 \ \mu m^2$. (b) Schematic of some of the capacitances in the measurement. (c) Example of drain-source current-voltage characteristics of a single-electron transistor at a refrigerator temperature of 50 mK shown for three values of gate voltage $C_{gs}V_g = eN_{SET} = 0$, 0.25 and 0.5 electrons. The arrow shows the drain voltage bias for optimal gain. (d) Dependence of the SET current with transparent quantum dot tunnel barriers on gate voltage for different drain-source voltage biases. Maximum peak-to-valley modulation amplitude is at SET $V_{ds} = E_c/e$.

Figure 1c shows the drain-source current-voltage relationship of the SET. It changes cyclically with the charge induced on the central island of the SET. Figure 1d displays the dependence of the current on the SET central island charge. For optimal charge sensitivity of the SET, we set the drain-source voltage at the onset of conduction for the maximum Coulomb blockade condition [13] (arrow in Fig. 1c), achieving a sensitivity of $1.2 \times 10^{-3} e/\sqrt{Hz}$ to the quantum dot charge.

Through application of a dc voltage V_g to the lead marked "gate" in Fig. 1a, charge can be drawn onto the dot as $eN = C_{gd}V_g$, where C_{gd} is the gate-dot capacitance. However, for zero temperature and for high tunneling barriers separating the dot from the leads, the charge on the quantum dot is quantized and can only change from n to $n + 1$ around points in gate voltage, where $N = (n + 0.5)$. The measured capacitance is $C_{meas} = e \partial \overline{n}/\partial V_g$, where $\overline{n}$ is the average number of electrons on the dot.

The capacitance line shape is measured by applying a small ac excitation (40 μV rms, 1 kHz) to the gate. This signal modulates the charge on the quantum dot by an amount that is a function of N and the coupling strength. The small ac modulation of the quantum dot

charge induces ac charge on the SET central island resulting in a current through the SET at the excitation frequency. Examples of the measured SET response as V_g is swept are shown in Fig. 2a for three different tunnel coupling strengths. The upper trace is obtained for $G = 1.65e^2/h$, where $\overline{n}$ deviates only slightly from N and the electrostatic potentials in the dot and the leads are nearly equal. A prominent feature of this curve is an oscillation with a period of 94 mV. This period arises due to an addition of one electron to the SET central island through a direct capacitance $C_{gs} = 1.7$ aF to the gate, modulating the gain of the SET.

The bottom trace in Fig. 2a is obtained for $G = 0.05e^2/h$. Here, the charge on the dot is well quantized and can change only in close proximity to points where $N = (n + 0.5)$. These points correspond to the sharp peaks in the trace, spaced with a mean period of 6.3 mV, yielding a gate-dot capacitance of $C_{gd} = 25$ aF. Notice that the large-period background oscillation has a larger amplitude compared with the upper traces in Fig. 2a. Between the peaks, the dot potential is effectively floating; charge cannot enter the dot from the reservoir to screen the ac gate potential. Thus, more charge is induced on the SET in response to the ac excitation on the gate because the ac coupling from the gate to the SET is augmented by a factor of $C_{gd}C_{ds}/C_{\Sigma}$. Here C_{ds} is the quantum dot-SET central island capacitance.

In general, the charge response on the SET central island, dQ_{SET}, to the ac excitation on the gate, dV_g, can be expressed as

$$dQ_{SET} = \left[(C_{gd} - C_{meas})\frac{C_{ds}}{C_{\Sigma}} + C_{gs} \right] dV_g. \quad (1)$$

The current through the SET directly reflects dQ_{SET}. Linear response of the SET is ensured because the ratio of C_{ds} to the total capacitance of the SET central island is about 0.05. Therefore, a change of charge of one electron in the quantum dot induces only $1/20^{th}$ of an electron
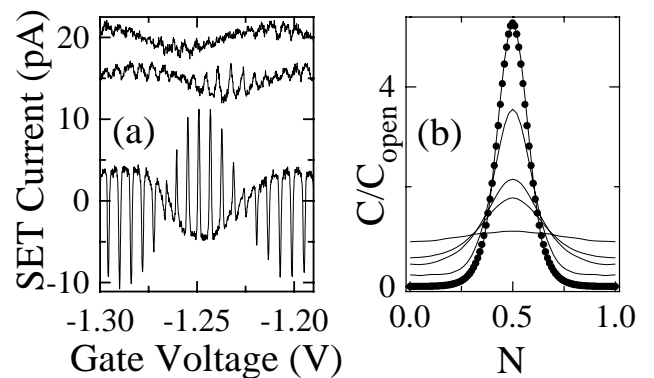

FIG. 2. (a) SET signal vs gate voltage for three values of point contact conductance. Top to bottom: $G = 1.65e^2/h$, $1.32e^2/h$, and $0.05e^2/h$. (b) Solid lines: Five capacitance peaks extracted from data; G is varied from $0.010e^2/h$ to $1.81e^2/h$. Closed circles: Derivative of the Fermi function for a temperature of 260 mK.

on the SET. Moreover, we obtain our capacitance line shapes at maximal gains of the SET where this small induced charge has minimal effect on the SET gain. The reverse effect of the SET on the quantum dot charge is also very small. The ratio C_{ds}/C_{Σ} is approximately 0.06, producing negligible feedback. Finally, the charge on the SET central island is poorly quantized since a finite source-drain voltage is applied to the SET. Using Eq. (1), we extract the quantum dot capacitance line shapes, $C_{meas}(V_g)$, from the raw data.

During measurement of the capacitance line shapes, point contact 2 is completely pinched off, and the dot is coupled to the leads only through point contact 1. To determine the conductance G of contact 1 in this regime, we perform the following procedure. The conductance of contact 1 is measured with 2 completely open. To account for the electrostatic coupling between contacts 1 and 2, we monitor the shift of conductance plateaus of contact 1 as 2 is being closed. We then extrapolate G to the regime of the capacitance measurement.

Figure 2b shows the evolution of the capacitance line shape with increased coupling strength. The nominal values of G are 0.010, 0.67, 1.09, 1.50, and $1.81e^2/h$. It is clear that as G increases and approaches $2e^2/h$, the capacitance peaks broaden and the Coulomb blockade oscillations diminish and disappear.

In the very weak coupling regime, the shape of the capacitance peak is determined simply by thermal broadening. Figure 2b shows good agreement between a peak measured with $G = 0.010e^2/h$ and a derivative of the Fermi-Dirac function for a temperature of 260 mK. We normalize this and all other line shape fitting functions by setting the integral over the line shape to correspond to the addition of one electron to the dot.

For larger tunnel barrier conductance, the capacitance line shape changes. In Figs. 3a, 3b, 3c, and 3d, we plot with open circles capacitance peaks that we obtained for nominal values of $G = 0.67$, 1.09, 1.50, and $1.81e^2/h$. We compared our capacitance peaks with expressions that have been previously used to fit conductance peaks. For example, Lorentzian lifetime broadening has been considered [6] for characterizing the charge smearing effects. In Figs. 3a, 3b, 3c, and 3d, we plot Fermi peaks broadened by convolution with Lorentzians for a temperature of 260 mK with energy level widths $\Gamma = 0.15U$, $0.32U$, $0.44U$, and $1.0U$. For these fits, we have used Γ as the single fitting parameter. In these and all other fits, the effect of the tails of neighboring peaks was included by adding seven independent peaks spaced in energy with a period of $2U$. The line shapes show significant deviations from the data. To avoid clutter, we have fit the Lorentzians to the valleys between our peaks. Nonetheless, fitting to the peak centers gives an equally poor result.

Previous measurements of charge fluctuations used a renormalized charging energy U^* to account for peaks broadened with a finite tunnel barrier conductance [8]. In
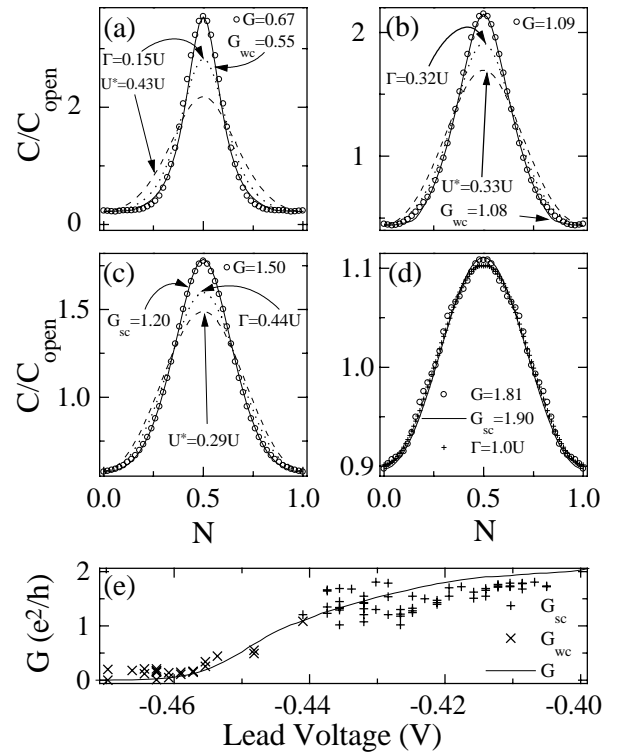

FIG. 3. (a) ○: data for $G = 0.67e^2/h$; solid line: fit to weak coupling (wc) theory with $G_{wc} = 0.55e^2/h$; dotted line: Lorentzian with $\Gamma = 0.15U$; dashed line: derivative of the Fermi function with $U^* = 0.43U$. (b) ○: data for $G = 1.09e^2/h$; solid line: wc fit with $G_{wc} = 1.08e^2/h$; dotted line: Lorentzian with $\Gamma = 0.32U$; dashed line: Fermi function with $U^* = 0.33U$. (c) ○: data for $G = 1.50e^2/h$; solid line: sc fit with $G_{sc} = 1.20e^2/h$; dotted line: Lorentzian with $\Gamma = 0.44U$; dashed line: Fermi function with $U^* = 0.29U$. (d) ○: data for $G = 1.81e^2/h$; solid line: sc fit with $G_{sc} = 1.90e^2/h$; +: Lorentzian with $\Gamma = 1.0U$. (e) Tunnel barrier conductance (solid line) vs tunnel barrier lead voltage. ×: conductance values obtained from fits with wc theory. +: conductance values obtained from fits with sc theory.

Figs. 3a, 3b, and 3c, we plot derivatives of the Fermi function with $U^* = 0.43U$, $0.33U$, and $0.29U$ for a temperature of 260 mK. Here, we have used U^* as the single fitting parameter. These line shapes clearly do not fit the data either.

Finally, we compare our experimental results to the theoretical treatment developed by Matveev [4,5]. The problem of interaction between the dot and the leads was solved in the limits of weak [3,4] and strong [5] coupling using either transmission or reflection of the tunnel barrier as a small parameter in perturbation theory. In both limits, the physics of charge fluctuations is related to spin fluctuations in the Kondo problem. Here, instead of the degeneracy of the two-spin states, there is a degeneracy between the dot states with n and $n + 1$ electrons. Similarly to the Kondo effect, the charge displays a logarithmic divergence around these degeneracy points at very low temperatures. As a result, the predicted capacitance line shape has more weight around the half-integer values of N in comparison with other theoretical treatments.

For weak coupling, this effect becomes pronounced at experimentally unattainable temperatures. Therefore, in the range of $G_{wc} \ll e^2/h$, it suffices to treat the tunnel coupling between the dot and the leads, G_{wc}, with the lowest orders in the perturbation theory. The expression for the capacitance far from the peak center is [3,4]

$$C = \frac{\partial Q}{\partial V_g} = a C_{gd} G_{wc} \left(\frac{h}{4\pi^2 e^2} \right)$$
$$\times \left(\frac{1}{0.5 - N} + \frac{1}{0.5 + N} \right). \quad (2)$$

Near the peak center, the calculation for nonzero temperatures yields an expression with a Fermi-Dirac component and an additive correction that is linearly dependent on G_{wc} [14]. In the theory [4], $a = 1$.

For strong tunneling, the theory [5] is based on perturbation in the reflection amplitude. The predicted capacitance is

$$C(N) = b C_{gd} r^2 \ln\left(\frac{1}{r^2 \cos^2 \pi N} \right) \cos 2\pi N + C_0. \quad (3)$$

The reflection coefficient r is related to the tunnel barrier conductance as $G_{sc} = 2(1 - r^2)e^2/h$, and in the theory $b = 2.27$. C_0 is constant with gate bias; its value is completely determined by G_{sc} through the requirement that the integral of $C(N)$ be normalized to one electron. C_0 is therefore *not* an independent parameter for fitting line shapes. To account for nonzero temperature, the singularity in (3) is cut off by replacing $r^2 \cos^2 \pi N$ with $r^2 \cos^2 \pi N + \frac{k_B T}{U}$. The corrected expression was used for the fits.

We fit every measured capacitance peak with the above described expressions using the conductance as the *single* fitting parameter with least squares optimization. In Fig. 3a and 3b, we show fits for weak tunneling with conductances of $G_{wc} = 0.55$ and $1.08 e^2/h$. These peaks are in excellent agreement with our data measured with tunnel barrier conductances of $0.67 e^2/h$ and $1.09 e^2/h$, respectively. The strong tunneling line shapes are shown in Figs. 3c and 3d. These figures show the strong tunneling calculations for conductances of $G_{sc} = 1.20$ and $1.90 e^2/h$, respectively. These line shapes agree well with our data, obtained with conductances of 1.50 and $1.81 e^2/h$. Figure 3d shows a capacitance peak for a nearly transparent tunnel barrier conductance. It is difficult to discern any significant differences between any of the theoretical calculations for these nearly sinusoidal line shapes. In contrast with theory, we found that G_{wc} corresponds well to the experimentally measured value if $a = 4$. For strong coupling, we found that the coefficient $b = 1$, to maintain the dependence of the capacitance line shape on G_{sc} in this limit. Similar discrepancies were observed elsewhere [15], but their cause is not known at this time.

Figure 3e shows the dependence of the tunnel barrier conductance on the voltage of the lead defining the tunnel barrier. We also plot the conductance values obtained

from theoretical fits in the weakly and strongly coupled regimes. These values have unexpectedly large fluctuations around the measured tunnel barrier conductance. They are seen consistently in all of our samples. Evidently, for a dot with a single point contact, the tunnel barrier conductance affecting the line shape differs from the conductance through the dot which does not display comparable fluctuations. In gate voltage sweeps for a fixed tunnel barrier conductance, the values of G_{wc} or G_{sc} are correlated over a few adjacent peaks. Theorists predict that such fluctuations can arise from quantum interference inside the dot and should therefore be highly sensitive to magnetic field. This is consistent with results from *conductance* experiments [16]. There are similar theoretical predictions for fluctuations in capacitance peaks [17]. However, we observed no effect of magnetic field for magnetic fluxes through the dot as high as 30 flux quanta.

*Current address: IBM Corp., San Jose, California 95193.
†Current address: Bell Labs, Lucent Technologies, Murray Hill, NJ 07974.
[1] R. C. Ashoori, Nature (London) **379**, 413 (1996); M. A. Kastner, Phys. Today **46**, No. 1, 24 (1993); L. P. Kouwenhoven *et al.,* Science **278**, 1788 (1997).
[2] M. Devoret and H. Grabert, in *Single Charge Tunneling,* edited by H. Grabert and M. Devoret, NATO ASI, Ser. B, Vol. 85 (Plenum, New York, 1992), p. 294.
[3] L. I. Glazman and K. A. Matveev, JETP **71**, 1031 (1990).
[4] K. A. Matveev, Sov. Phys. JETP **72**, 892 (1991).
[5] K. A. Matveev, Phys. Rev. B. **51**, 1743 (1995).
[6] E. B. Foxman *et al.,* Phys. Rev. B **47**, 10020 (1993).
[7] A. Furusaki and K. A. Matveev, Phys. Rev. Lett. **75**, 709 (1995).
[8] L. W. Molenkamp, K. Flensberg, and M. Kemerink, Phys. Rev. Lett. **75**, 4282 (1995); K. Flensberg, , Phys. Rev. B. **48**, 11156 (1993).
[9] F. R. Waugh *et al.,* Phys. Rev. Lett. **75**, 705 (1995).
[10] K. A. Matveev, L. I. Glazman, and H. U. Baranger, Phys. Rev. B **54**, 5637 (1996).
[11] D. Berman *et al.,* J. Vac. Sci. Technol. B **15**, 2844 (1997).
[12] T. A. Fulton and G. J. Dolan, Phys. Rev. Lett. **59**, 109 (1987).
[13] P. Lafarge *et al.,* Z. Phys. B. **85**, 327 (1991).
[14] H. Grabert, Phys. Rev. B. **50**, 17364 (1994); K. A. Matveev (private communication).
[15] D. S. Duncan (private communication).
[16] R. A. Jalabert, A. D. Stone, and Y. Alhassid, Phys. Rev. Lett. **68**, 3468 (1992); A. M. Chang *et al.,* Phys. Rev. Lett. **76**, 1695 (1996); J. A. Folk *et al.,* Phys. Rev. Lett. **76**, 1699 (1996).
[17] I. L. Aleiner and L. I. Glazman, Phys. Rev. B **57**, 9608 (1998); A. Kaminsky, I. L. Aleiner, and L. I. Glazman, cond-mat/9802159.